C-6-7

Conduction Mechanisms for Off-State Leakage Current of Schottky Barrier Thin-Film Transistors (SBTFT)

Kuan-Lin Yeh[1], Horng-Chih Lin[2,*], Rou-Gu Huang[1], Ren-Wei Tsai[1], and Tiao-Yuan Huang[1,2]

[1]Institute of Electronics, National Chiao Tung University, 1001 Ta-Hsueh Rd., Hsin-Chu 300,Taiwan
[2] National Nano Device Laboratories, 1001-1 Ta-Hsueh Rd., Hsin-Chu 300,Taiwan *FAX: 886-3-5722715; Email: hclin@ndl.gov.tw

1. Introduction

We have recently proposed and demonstrated a novel poly-Si Schottky barrier thin-film transistor (SBTFT) featuring Co-silicided source/drain and a metal field-plate (i.e., sub-gate) lying over the passivation oxide. No source/drain ion implantation is required in the device fabrication. In addition, the device is capable of ambipolar operation, which results in significant mask savings in CMOS process integration. Excellent on/off current ratios of over 10^6 have been achieved simultaneously for both n- and p-channel operations on the same device [1][2]. In addition, the GIDL (gate-induced drain leakage)-like off-state leakage current that has plagued previous SBTFT devices (i.e., without field-plate) could be completely suppressed [2]. In this work, we carried out further study on characterizing the off-state leakage of the devices at different temperatures. Based on the obtained results, the off-state leakage conduction mechanisms are discussed and identified for the first time.

2. Device Structure

Figures 1(a) and (b) show the cross-sectional views for devices with the proposed FID and the conventional structure, respectively. Detailed fabrication flow and process conditions could be found in our previous works [1][2]. After the metal-pad patterning, the devices received a plasma treatment at 250 °C in NH_3 for one hour before measurement. It is worthy to note that the metal sub-gate was formed during the regular metal patterning, so no extra process steps were required. During device operation, a proper fixed voltage is applied to the field-plate to form a field-induced drain (FID) layer under the field-plate region. So depending on the polarity of the field-plate bias, the device can be set for n- and p-channel operations with positive and negative field-plate biases, respectively.

3. Results and Discussion

Figure 2 shows the I_D-V_G characteristics measured at different temperatures for an SBTFT with conventional structure. It can be seen clearly that the leakage current increases with increasing $|V_{GD}|$ in the off state. The results for an SBTFT with FID are shown in Fig.3. The leakage shows only weak dependence on $|V_{GD}|$, in strong contrast to that shown in Fig.2. The corresponding Arrhenius plots for p-channel and n-channel operations ($|V_G| = 0$ and 4.5 V) are shown in Figs.4 and 5, respectively. The extracted activation energies (E_A) of I_D for the device with conventional structure are smaller than that of the FID device. In addition, E_A decreases with increasing $|V_G|$, though the effect is much more pronounced for the device with conventional structure.

Band diagrams illustrated in Fig.6 are used to explain the above results. In the figure, we concentrate only on the n-channel operation, although similar results could also be deducted for p-channel operation. For the device with conventional structure, the field emission and thermionic emission of holes from the drain are presumably the primary conduction mechanisms of off-state leakage (Fig.6(a)). Under the condition when the field strength is weak, the thermionic emission would dominate the conduction while the activation energy for the leakage will be closer to the barrier height. When the field strength increases, the field emission will become significant. This is evidenced from Figs.4 and 5 that E_A for the conventional device decreases when $|V_G|$ increases. On the other hand, when FID scheme is implemented, as shown in Fig.6(b), the FID would pull the high-field region in the channel away from the drain side. As a result, thermionic emission would be the major conduction mechanism in the off sate. In addition, the high bias applied on the field-plate (e.g., 50 V) would shift the Fermi level in the offset channel region closer to the conduction band edge, thus raises the barrier height for thermionic emission. This explains why E_A of FID devices is higher than that of the conventional structure.

Figure 7 shows E_A as a function of V_G for both p-channel and n-channel operation of the devices. For FID devices, it can be seen that E_A is essentially independent of V_G in the off state for both p-channel and n-channel operation. This confirms our deduction that thermionic emission is the dominant mechanism responsible for the leakage. On the other hand, significant lowering in E_A as $|V_{GD}|$ increases is observed for devices with the conventional structure, indicating that field emission process will dominate the leakage as the field strength becomes high.

4. Conclusions

With the aids of FID in the novel SBTFT structure we proposed, the high field region in the off state would be pulled away from the drain side, thus the GILD-like leakage current could be effectively suppressed. While the conventional SBTFT depicts large GILD-like leakage current and low on/off current ratio of less than 10^3, the new device depicts GILD-free characteristics with on/off current ratio as high as 10^6 for both n-channel and p-channel modes of operation on the same device [1][2]. The superior characteristics, together with its inherent ambipolar capability, implantless process, silicided source/drain, low thermal budget, and ultra-low mask-count in CMOS integration, make the new device very promising for future large-area electronic applications.

References:
[1] H. C. Lin *et al*, in *Tech. Dig. IEDM* (2000), p.857.
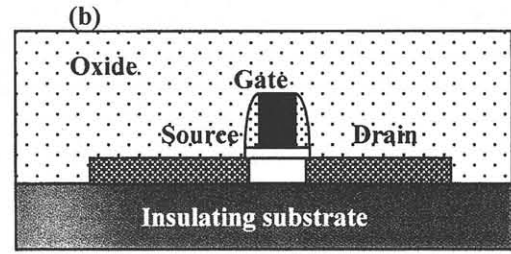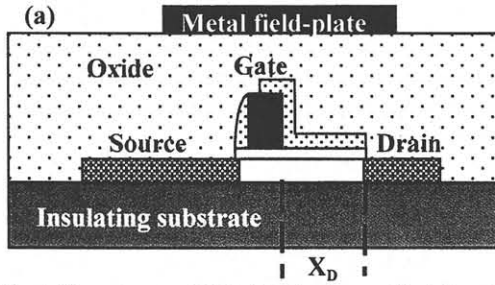[2] H. C. Lin *et al*, IEEE EDL- **22**, pp.179-181, (2001)

Fig.1 Structures of SBTFT devices with (a) and without (b) the field-plate. X_D in (a) is the length of the offset region in the channel.
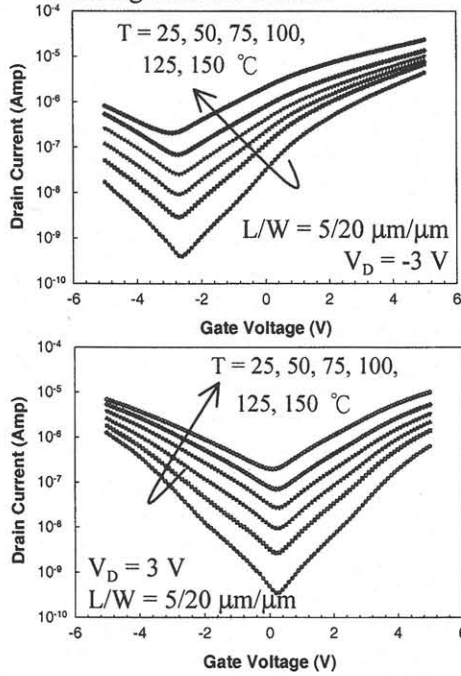

Fig.2 I_D-V_G characteristics for p- (top) and n- (bottom) channel operation of SBTFT with conventional structure.
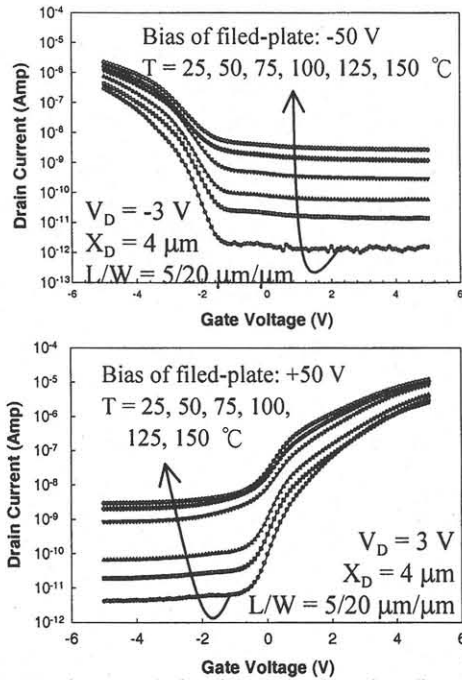

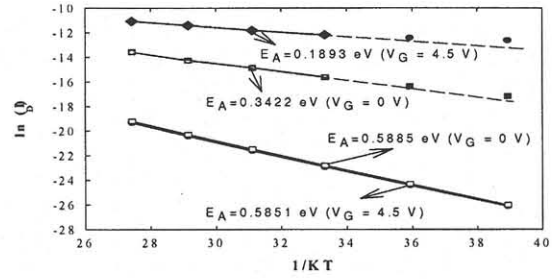Fig.3 I_D-V_G characteristics for p- (top) and n- (bottom) channel operation of SBTFT with FID.

Fig.4 Arrhenius plots for p-channel operation of SBTFTs. (Empty symbols: FID; filled symbols: conventional structure)
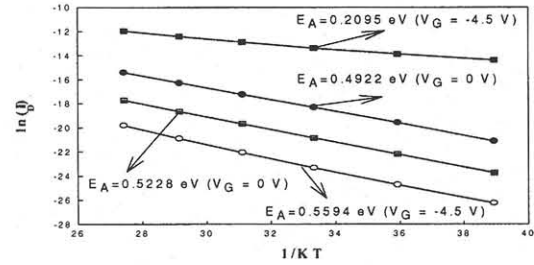

Fig.5 Arrhenius plots for n-channel operation of SBTFTs. (Empty symbols: FID; filled symbols: conventional structure)
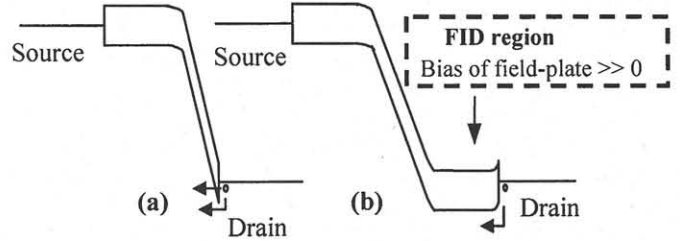

Fig.6 Band diagrams for n-channel operation of SBTFTs with (a) conventional and (b) FID structures. ($V_G \sim 0$)
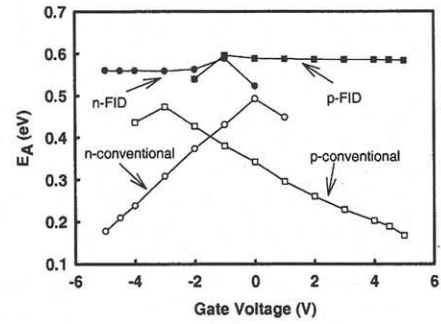

Fig.7 E_A v.s. V_G for p- (V_D = -3 V) and n- (V_D = 3 V) channel operation of SBTFTs with FID or conventional structure.